

STRUCTURE AND CRYSTALLOGRAPHIC TEXTURE IN THE Cu-Cr-Ag ALLOY SUBJECTED TO SEVERE PLASTIC DEFORMATION

R.K. Islamgaliev^{1,2}, V.D. Sitdikov¹, K.M. Nesterov¹ and D.L. Pankratov²

¹Ufa State Aviation Technical University, K.Marks Str., 12, 450000 Ufa, Russia

²Kazan Federal University, Kremlevskaja Str., 18, 420008 Kazan, Russia

Received: September 02, 2014

Abstract. In this paper the effect of severe plastic deformation (SPD) on the structure and crystallographic texture in the Cu-Cr-Ag copper alloy have been investigated. In ultrafine-grained (UFG) samples processed by high pressure torsion (HPT), equal channel angular pressing (ECAP) and ECAP-Conform (ECAP-C) the average size of grains and precipitates was determined. Experimental pole figures (PF) have been obtained and the relevant crystallographic texture was evaluated. The effect of dynamic aging in the Cu-Cr-Ag alloy leading to improvement of strength and electrical conductivity was observed.

1. INTRODUCTION

It is known that the Cu-Cr-Ag alloy is an attractive material for various electrical applications because of enhanced strength and good electrical conductivity [1,2]. The enhanced strength in coarse-grained Cu-Cr-Ag alloy is attributed to precipitation hardening whereas the good electrical conductivity is due to low solubility of chromium in copper.

At the same time one can expect that grain refinement will lead to improving tensile strength at room temperature without significant loss in electrical conductivity.

In recent years for grain refinement in metals and alloys the various methods of severe plastic deformation (SPD) have been developed [3-5].

The SPD treatment is based on the application of large shear deformations at high pressures and low homologous temperatures and it is accompanied by the active crystallographic slip leading to a reorientation of the grains and the formation of crystallographic texture [6].

In particular, a strong preferential orientation of the crystallites typical for simple shear texture has been found in pure Cu subjected to initial stages of SPD processing [6]. Therefore one can expect that the increase of accumulated strain in SPD processing will lead to changes in the texture influencing on strength of the UFG material.

An important role in hardening of the Cu-Cr-Ag alloy plays also the dispersed particles precipitating after quenching and aging [1]. Aging of these alloys is carried out at temperatures above the beginning of grain growth in the UFG pure copper. Therefore precipitation of particles may promote not only hardening, but also thermal stability of grains during heating.

On the other hand, in addition to improving strength in the copper alloy there is another important task, namely, to avoid loss of electrical conductivity.

It is known, that electrical resistance of metallic materials increases in the presence of defects of

Corresponding author: R.K.Islamgaliev, e-mail: saturn@mail.rb.ru

crystal lattice (alloying elements, impurities, dislocations, particles, grain boundaries) [1,7-9].

For example, alloying of copper with chromium to 0.4-1.0 wt.% leads to a decrease in electrical conductivity at room temperature by 16% [10]. Whereas the formation of an average grain size of 150 nm by HPT enhances the electrical resistivity at 20°C less than 5% [11]. For comparison, the contribution of dislocations to electrical resistivity at a density of 10^{11} cm^{-2} is $2.3 \times 10^{-10} \text{ Ohm} \times \text{m}$, i.e. value of about 1.3% of the electrical resistivity of pure copper [12].

From these estimates it follows that the contribution of alloying elements to electrical resistivity at room temperature is significantly higher in comparison with the grain boundaries, dislocations and vacancies. Therefore, reducing the content of alloying elements in the crystal lattice by their redistribution to the grain boundaries could contribute to the improvement of electrical conductivity.

One possible way of improving the strength and electrical conductivity is to provide UFG structure in which atoms of the alloying elements will be located in the form of precipitates at grain boundaries and triple junctions, wherein the dislocation density would be low.

The formation of such structure is possible due to an effect of dynamic aging observed in UFG materials [13] as a result of lowering the activation energy of the grain boundary diffusion in UFG materials [14].

Thus, the aim of this paper is to fabricate the UFG structure in the Cu-Cr-Ag alloy using SPD processing to analyze structural factors leading to improving strength and electrical conductivity.

2. EXPERIMENTAL

The Cu-Cr-Ag alloy manufactured by Wieland (Germany) was selected as initial material for investigations. The results of optical emission analysis performed by the spectrometer Bruker Q4 TASMAN are shown in the Table 1.

In the first step the initial Cu-Cr-Ag alloy was coated with liquid glass and solid solution treated at 1050 °C for 1 h with water quenching. Then the disks with a diameter of 20 mm and a thickness of 1.5 mm were subjected to high pressure torsion

(HPT) at various temperatures through $N=10$ turns at pressure 6 GPa using constrained anvils [5].

Processing by equal-channel angular pressing (ECAP) was performed using 8 passes on the route Bc with the angle of intersection of the channels equal to 90 degrees at the temperatures of 20 °C and 300 °C on samples of 10 mm diameter and 60 mm long [4].

ECAP-C was carried out at the temperatures of 20 °C and 300 °C using square cross-section of the working channel $12 \times 12 \text{ mm}^2$ and the angle of intersection of the channels 120 degrees [15].

The microstructure of the alloy was characterized using JEM-2100 transmission electron microscope (200 kV TEM). TEM foils, discs with a diameter of 2.3 mm were punched from slices of the ECAP-processed samples. Then they were mechanically ground to a thickness of 0.15 mm, and finally double-jet electropolished to perforation using an electrolyte consisting of 920 ml H_2O , 70 ml H_3PO_4 , 15 ml $\text{C}_3\text{H}_5(\text{OH})_3$.

The analysis of texture in the Cu-Cr-Ag alloy was performed on the DRON-3M diffractometer equipped with an automatic texture attachment using $\text{Cu } K_{\alpha 1}$ radiation in reflection geometry at the radial angles from 0 to 75° and azimuthal angle from 0° to 360°. The diameter of the irradiated region corresponded to 0.6 mm. In the case of ECAP and ECAP-C the study was carried out in the geometric center of the longitudinal section of the workpiece, as in the case of HPT in the plane of the disk. Results of experimental studies were presented in the form of complete pole figures (PF) in the shear plane, calculated using the software package LaboTEX (www.labosoft.com.pl).

The measurements of the Vickers microhardness were made using a Micromet 5101 device with loads of 100 g for 10 s along the diameter of the HPT samples and cross-section of the ECAP samples.

The electrical conductivity of the alloy at the temperature of 20 °C was measured using eddy current method. At least 20 measurements were taken and the average values and their standard deviation were calculated. Tensile specimens with dimension $0.5 \times 1 \times 4 \text{ mm}^3$ were machined from the processed bars. Tensile tests were carried out using a specially designed testing machine [16]. Tensile specimens were deformed to failure at room temperature

Table 1. Chemical composition of the Cu-Cr-Ag alloy.

Element	Cr	Ag	Fe	P	Si	Cu
wt. %	0.5	0.12	0.06	0.06	0.05	balance

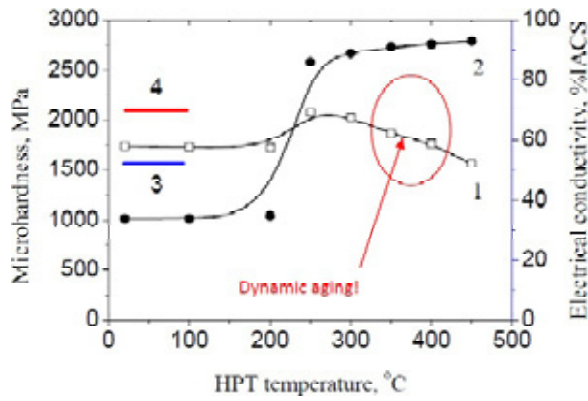


Fig. 1. Dependence of microhardness (1) and electrical conductivity (2) on the HPT temperature; (3), (4) - levels of microhardness and electrical conductivity in coarse-grained samples subjected to standard treatment.

with constant cross-head speed corresponding to the initial strain rate of 10^{-3} s^{-1} . Three tensile specimens with gage length of 4 mm and a cross-section of 1.0 mm \times 0.7 mm were tested and the results obtained were found to be reproducible.

3. RESULTS

It is known that the structure of metallic materials depends strongly on the regimes of SPD processing. In particular, the SPD temperature plays an important role because it could affect on the grain refinement, recrystallization and phase transformations [17].

Therefore, to select the optimal SPD temperatures the dependence of structural sensitive parameters (microhardness, electrical conductivity) on the HPT temperature has been investigated (Fig. 1).

Application of HPT at 20 °C resulted in an increase in the microhardness and decrease in electrical conductivity as compared with the coarse-grained sample subjected to solid solution treatment followed by quenching and aging at 500 °C for 30 min (Fig. 1).

After HPT processing at 300 °C we have observed the combination of enhanced microhardness and electrical conductivity in comparison with the samples processed at 20 °C (Fig. 1). It should be noted that aging in coarse-grained samples starts

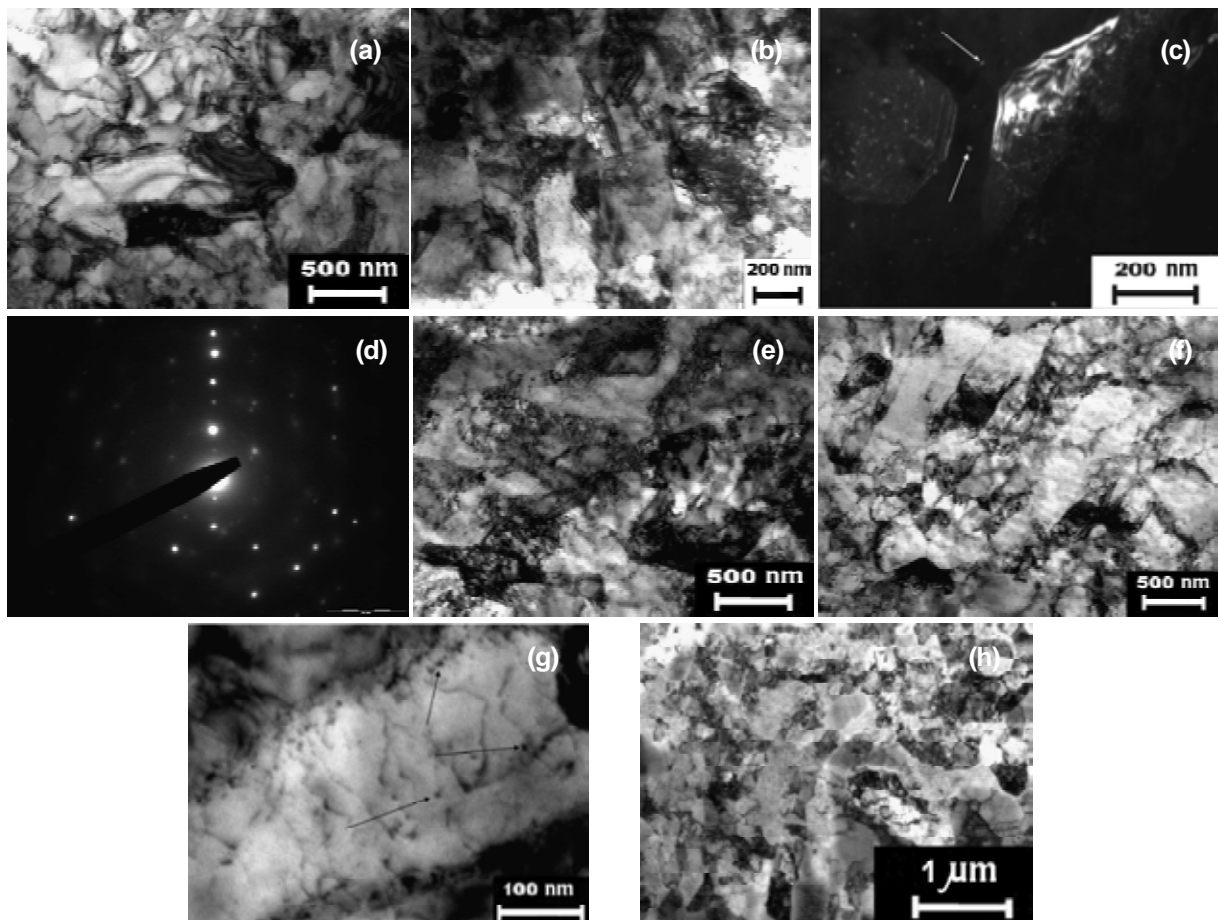


Fig. 2. Typical microstructures: (a) HPT at 20 °C; (b,c,d) HPT at 300 °C; (e) ECAP at 20 °C; (f,g) ECAP at 300 °C; (h) ECAP-C at 300 °C; (a, b, e, f, g, h) bright field image; (c) dark field image; (d) electron diffraction pattern from particles observed in (c); (c, g) arrows indicate particles.

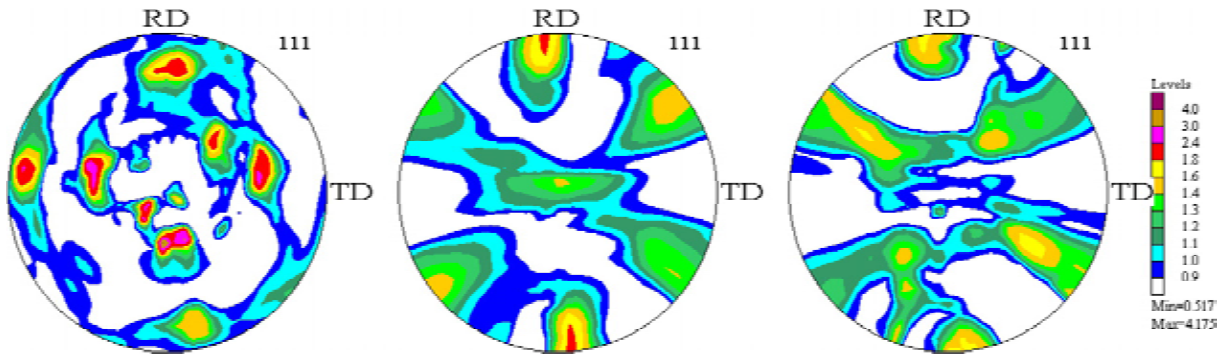


Fig. 3. PF (111) for the Cu-Cr-Ag alloy: (a) initial quenched condition; (b) after HPT at 20 °C; (c) after HPT at 300 °C.

usually at 400 °C. However the peak of microhardness in ultrafine-grained samples was achieved at 300 °C. It means that HPT leads not only to grain refinement, but also to dynamic aging at lower temperatures, because the temperature of aging in ultrafine-grained (UFG) material was reducing by 100 °C. Thus, the greatest interest for structural investigations are the UFG samples processed by SPD at temperatures of 20 °C and 300 °C. As a consequence, they were chosen for further analysis by transmission electron microscopy and X-ray diffraction.

Careful TEM studies have shown that the alloys processed by HPT at 20 °C exhibit a very homogeneous UFG structure (Fig. 2a) with a mean grain size of about 200 nm. No visible precipitates have been detected after this treatment. At the same time in addition to a grain size of 200 nm (Fig. 2b) we observed the precipitation of the Cr particles with a size of 10 nm directly after HPT processing at 300 °C (Figs. 2c and 2d). It should be noted that precipitation of the Cr particles in the Cu-Cr-Ag alloy has been observed also after standard treatment by quenching and aging in [1,2].

For the formation of UFG structure in samples of bigger size the method of equal-channel angular

pressing has been used. Taking into account the experimental data on the dynamic aging observed in the HPT samples (Fig. 1, Fig. 2c), the ECAP was also carried out at temperatures of 20 °C and 300 °C. From TEM investigations the average grain size of these samples was 330 nm (Fig. 2e) and 400 nm (Fig. 2f), respectively. In addition the precipitates of Cr particles with a size of 5 nm have been observed too (Fig. 2g).

The samples subjected to ECAP-C at a temperature of 300 °C were characterized by a strong grain refinement to an average grain size of 400 nm (Fig. 2h). They exhibit also similar chromium particles with an average size of about 5 nm.

The initial quenched material has shown a random distribution of texture maxima (Fig. 3a). Application of HPT at 20 °C resulted in the formation of texture components A_1^* , A_2^* , \bar{A} , \hat{A} , and C (Fig. 3b) typical for simple shear texture (Fig. 4a) [6,18].

After HPT at 300 °C the combination of cubic texture component $\{001\}\langle 100 \rangle$ and the simple shear texture was observed (Figs. 3c and 4b). The latter indicates to activation of recrystallization during HPT processing at enhanced temperature, because 300 °C is substantially higher than 175 °C from which the grain growth in the HPT copper begins [20].

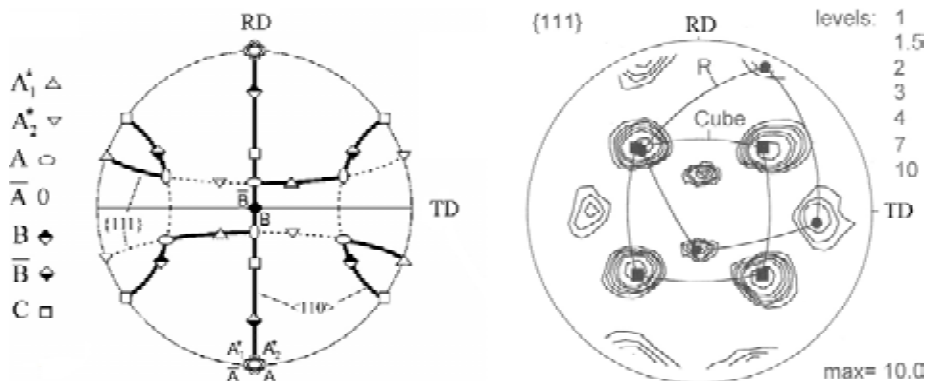


Fig. 4. (a) The ideal texture components in pure copper corresponding to simple shear; (b) texture after recrystallization, replotted results from [6,19].

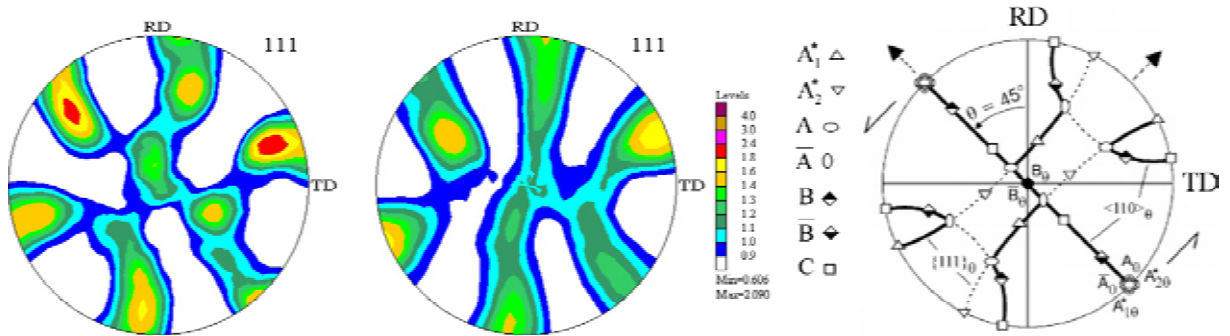


Fig. 5. PF (111) for the Cu-Cr-Ag alloy after eight ECAP passes: (a) at $T = 20$ °C; (b) at $T = 300$ °C. (c) The ideal orientations of simple shear texture after rotation at an angle of 45° counterclockwise, replotted results from [18].

Weakness of the texture components \bar{A} and A after increase in strain was observed also in [18,21] where it is explained by development of dynamic recrystallization. In this case, component B was more stable to grain growth than component A .

After eight ECAP passes at $T = 20$ °C on the PF (111) one can see 8 distinct maxima (Fig. 5a). Six texture maxima are symmetrically located on the periphery of the PF and the two near the center of the PF. These maxima as in the case of HPT correspond to components $A\{111\} \langle uvw \rangle$, $B\{hkl\} \langle 110 \rangle$ and $C\{001\} \langle 110 \rangle$ typical for simple shear texture. This crystallographic texture can be described by the ideal orientations (Fig. 5c) with respect to rotation of ideal orientations of simple shear at an angle of 45 degrees counterclockwise.

Crystallographic texture of the Cu-Cr-Ag alloy subjected to ECAP at 300 °C is identical and is characterized by the dominant components of simple shear texture $\{110\} \langle 111 \rangle$ (Figs. 5a and 5b). At the same time there is some weakening of texture components A_1^* , A_2^* , \bar{A} , A , and C . In addition, a shift in the orientation B in the fiber of ($\langle 110 \rangle //$ shear direction) from the ideal orientation A_2^* to the ideal

orientation of C was observed. All this points to the activation of recrystallization processes [19,22].

PF (111) after eight passes ECAP-K at $T = 300$ °C was characterized by two main maxima positioned at the periphery of the PF at angles approximately equal to 60° with respect to the axis of RD (Fig. 6a). Location of maxima is similar to what is observed in conventional ECAP with the angle of intersection of the channels 120° . In this case, the texture can be characterized by the ideal orientations $A\{111\} \langle uvw \rangle$, $B\{hkl\} \langle 110 \rangle$ and $C\{001\} \langle 110 \rangle$ corresponding to simple shear texture (Fig. 6b). Maxima indicate to the activity of dislocation glide on the $\{111\}$ and $\{001\}$ slip planes. At the same time the observed shift of orientations A and \bar{A} to orientation B and \bar{B} indicates to development of recrystallization processes.

3. DISCUSSION

TEM investigations (Fig. 2) testify that the application of HPT, ECAP, and ECAP-K to the Cu-Cr-Ag alloy leads to the formation of UFG structure with an average grain size of less than 400 nm. The dif-

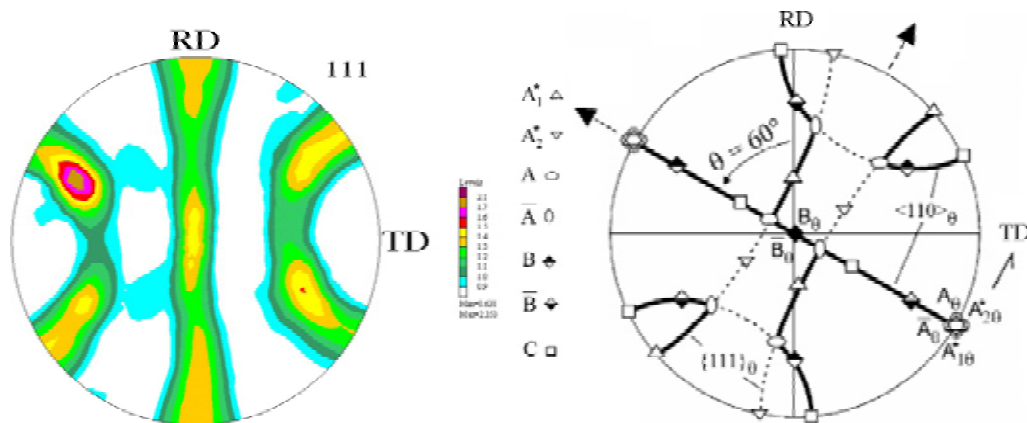


Fig. 6. (a) PF (111) for the Cu-Cr-Ag alloy after eight ECAP-C passes at $T = 300$ °C. (b) The ideal orientations of simple shear texture after rotation at an angle of 60° counterclockwise.

Table 2. Parameters of the Cu-Cr-Ag alloy after various treatments.

Treatment	Grain size, nm	Size of precipitates, nm	Micro-hardness, MPa	Electrical conductivity, %IACS	UTS, MPa	Ductility, %
HPT 20	200	-	1740	34	530	13
HPT 300	200	10	2020	93	590	12
ECAP 20	330	-	1470	25	440	12
ECAP 300	400	5	1450	30	390	12
ECAP-C 300	400	5	1470	25	480	18

ference in a grain size observed between HPT, ECAP and ECAP-K samples can be explained by variation in the level of shear deformation imposed on the samples.

According to the Cu-Cr phase diagram [22] the chromium particles precipitate in the coarse-grained samples after quenching and aging at a temperature of 450-500 °C [1,2]. However, a decrease in the temperature of the particles precipitation to 300 °C in the UFG samples has been observed as a result of dynamic aging during SPD (Fig. 2c) [23]. This effect is associated with reduced activation energy of the grain boundary diffusion [14] and a large volume fraction of grain boundaries in the UFG samples. In this case, the smaller particle size (5 nm) in the ECAP samples compared to the size of the particles (10 nm) in the HPT samples processed at the same temperature of 300 °C, can be due to a lower degree of shear deformation and lower pressures used in the ECAP.

Although it is known that the application of SPD leads to an increase in the microhardness in various metals and alloys as a result of strong grain refinement [24] nevertheless, in the present work a maximum microhardness has been observed after HPT at temperatures of 250-300 °C (Fig. 1). This is caused by the additional contribution of the dispersion hardening due to precipitation of particles as a result of dynamic aging (Fig. 2c). Decrease in microhardness at higher temperatures HPT (Fig. 1) is caused by a decay of supersaturated solid solution and coarsening of precipitates.

Experimental data show that the highest values of microhardness of 1740 MPa and tensile strength of 590 MPa exhibit the samples processed by HPT at 300 °C (Table 2). Higher strength is the result of a small grain size of 200 nm and the contribution of dispersion hardening due to the presence of the chromium precipitates with a size of 10 nm. The other samples show lower strength because of the larger grain size (ECAP 20, ECAP 300, ECAP-K 300) or the lack of visible dispersed particles of chromium (HPT 20, ECAP 20).

There was also a significant difference in tensile strength between the samples processed by ECAP and ECAP-C at the same temperature of 300 °C (Table 2). Both of these samples have same grain size and a size of particles but, nevertheless, the tensile strength in the ECAP-C samples was noticeably higher. This can be explained by the difference in the crystallographic texture of the samples. In particular, the texture maxima deviations of 45 and 60 degrees relative to the axis of the RD, observed on the pole figures (Fig. 5b, Fig. 6a). In turn, these deviations of 45 and 60 degrees can be caused by application of the installations with different angles of intersection of the channels 90 and 120 degrees, respectively. It should be noted that the effect of texture on strength of ECAP samples is already known in the literature [25].

The highest electrical conductivity of 93% IACS was observed in the HPT samples processed at 300 °C. This was facilitated by a decrease in the content of alloying element chromium in the crystal lattice inside the grains by their redistribution to the grain boundaries during dynamic aging at 300 °C under conditions of shear deformation and high pressure. In addition, there is a recovery of the defect structure at elevated temperatures, which is accompanied by a decrease of the density of dislocations and the reduction of internal stresses. Both of these factors, namely, the redistribution of the alloying elements and the recovery of the defect structure contribute to the increase of electrical conductivity. Whereas a supersaturated solid solution and the defect structure in the HPT samples processed at 20 °C resulted in significantly lower electrical conductivity of 34% IACS.

Another interesting feature is the significant difference in electrical conductivity between the samples processed by ECAP and ECAP-C at the same temperature of 300 °C (Table 2), although they exhibit similar structures with the same size of grains and particles. This effect can be explained by the difference in the location of the main texture maxima

Table 3. Parameters of the UFG samples of the Cu-Cr-Ag alloy after additional annealing.

Treatment	Grain size, nm	Size of precipitates, nm	Micro-hardness, MPa	Electrical conductivity, %IACS	UTS, MPa	Ductility, %
HPT 20 + 450 °C, 30 min	300	10	2170	81	845	9
HPT 300 + 450 °C, 30 min	300	10	1820	92	600	13
ECAP 20 + 500 °C, 120 min	500	10	2010	85	660	11
ECAP 300 + 500 °C, 120 min	500	10	1950	85	570	11

in the pole figures. Note that the effect of the crystallographic texture on electrical conductivity of pure copper is already known in the literature [26].

Experimental data presented above in Fig. 1, shows that the strength of the UFG samples can be improved by heat treatment in the temperature range 450-500 °C leading to additional precipitation of chromium particles. In this paper, the greatest effect of additional heat treatment was observed in the UFG samples processed by HPT at 20 °C and annealed at 450 °C for 30 min (Table 3). In these samples the enhanced strength up to 845 MPa with ductility of 9% and electrical conductivity of 81% IACS was achieved (Table 3) due to a small grain size of 300 nm and additional precipitation of chromium particles.

4. CONCLUSIONS

Thus from the results obtained one can make the following conclusions.

1. Application of various SPD treatments (HPT, ECAP, ECAP-C) to the Cu-Cr-Ag alloy leads to the formation of the UFG structure with an average grain size less than 400 nm, depending on the used scheme and temperature of processing.
2. The effect of dynamic aging in the Cu-Cr-Ag alloy leading to improvement of strength and electrical conductivity has been observed.
3. Crystallographic texture in the UFG samples of the Cu-Cr-Ag alloy processed by various SPD treatments (HPT, ECAP, ECAP-C) has similarities and differences. Common feature is the formation of simple shear texture described by components A_1^* , A_2^* , A , \bar{A} , B , \bar{B} , and C associated with the implementation of the shear deformation. In this case, the slip system $\langle 110 \rangle \{111\}$ are active in all three of the above schemes SPD. The difference in texture is caused by variation in temperature, strain and

pressure applied in the used SPD schemes resulting in a change of the slip systems activity (change pole density in the PF).

4. Formation of the UFG structure and dispersed chromium particles contributes to enhanced ultimate tensile strength of 845 MPa with electrical conductivity of 81% IACS, which much higher in comparison with coarse-grained Cu-Cr-Ag alloy demonstrated after standard treatment 430 MPa and 68% IACS, respectively.

ACKNOWLEDGEMENT

The work is performed according to the Russian Government Program of Competitive Growth of Kazan Federal University. One of the authors (K.M.) would like to acknowledge the support by the Russian Ministry of Education and Science within the basic part of the program for universities.

REFERENCES

- [1] C.Watanabe, R.Monzen and K.Tazaki // *J. Mat. Sci.* **43** (2008) 813.
- [2] S.G.Jia, M.S.Zheng, P.Liu, F.Z.Ren, B.H.Tian, G.S.Zhou and H.F.Lou // *Mat. Sci. Eng. A.* **419** (2006) 8.
- [3] R.Z.Valiev, R.K.Islamgaliev and I.V.Alexandrov // *Progr. Mater. Sci.* **45** (2000) 103.
- [4] R.Z.Valiev and T.G.Langdon // *Progr. Mater. Sci.* **51** (2006) 881.
- [5] A.P.Zhilyaev and T. G. Langdon // *Progr. Mater. Sci.* **53** (2008) 893.
- [6] I.J Beyerlein and L. S. Tóth // *Prog Mater Sci.* **54**, 4 (2009) 427.
- [7] Y.Champion and Y.Brechet // *Adv. Eng. Mat.* **12**, 8 (2010) 798.
- [8] K.Hanazaki, N.Shigeiri and N.Tsuji // *Mat. Sci. Eng. A.* **527** (2010) 5699.

- [9] N.Takata, S.H.Lee and N.Tsuji // *Mater. Letters*. **63** (2009) 1757.
- [10] O.Osintsev and V.N.Fedorov, *Copper and copper alloys* (Machinostroenie, Moscow, 2004), In Russian.
- [11] R.K.Islamgaliev, K.Pekala, M.Pekala and R.Z.Valiev // *Phys.stat.sol. (a)*. **162** (1997) 559.
- [12] O.A.Shmatko and Yu.V.Usov, *Structure and properties of metals and alloys. Electric and magnetic properties of metals* (Naukova Dumka, Kiev, 1987).
- [13] R.Z.Valiev, M.Yu.Murashkin, E.V.Bobruk and G.I.Raab // *Mater. Transactions* **50** (2009) 87.
- [14] Yu.R.Kolobov and R.Z.Valiev, *Grain-boundary diffusion and properties of nanostructured materials* (Nauka, Novosibirsk, 2001).
- [15] G.I.Raab, R.Z.Valiev, D.V.Gunderov, T.C.Lowe, A.Misra and Y.T.Zhu // *Mat. Sci. Forum* **584-586** (2008) 80.
- [16] O.B.Kulyasova, R.K.Islamgaliev and R.Z.Valiev // *Physics of Metals and Metallography* **100**, 3 (2005) 277
- [17] B.Mingler, O.B.Kulyasova, R.K.Islamgaliev, G.Korb, H.P.Karntaler and M.J.Zehetbauer // *J. Mat. Sci.* **42**, 5 (2007) 1477.
- [18] I.V.Alexandrov, A.A.Dubravina and M.V.Zhilina // *Russian Metallurgy (Metally)* **6** (2005) 469.
- [19] U.F.Kocks, C.N.Tome and H.R.Wenk, *Texture and anisotropy: preferred orientations in polycrystals and their effect* (Cambridge University Press, Cambridge, 1998).
- [20] N.M.Amirkhanov, J.J.Bucki, R.K.Islamgaliev, K.J.Kurzydowski and R.Z.Valiev // *Journal of Metastable and Nanocrystalline Materials* **9** (2001) 21.
- [21] N.A.Enikeev, E.Schafler, M.J.Zehetbauer, I.V.Alexandrov and R.Z.Valiev // *Mater. Sci. Forum* **584 - 586** (2008) 367.
- [22] D.J.Chakrabarti and D.E.Launglin // *Bulletin of Alloy Phase Diagrams* **5(1)** (1984) 59.
- [23] R.K.Islamgaliev, K.M.Nesterov, J.Bourgon, Y.Champion and R.Z.Valiev // *J. Appl. Phys.* **115** (2014) 194301.
- [24] R.K.Islamgaliev, N.F.Yunusova, I.N.Sabirov, A.V.Sergeeva and R.Z.Valiev // *Mat. Sci. Eng. A.* **319-321** (2001) 874.
- [25] D.R.Nugmanov and R.K.Islamgaliev // *Reviews on Advanced Materials Science* **31** (2012) 157.
- [26] A.A.Bryuhanov and V.V.Usov // *Physics of Metals and Metallography* **4** (1992) 125, In Russian.